ARL-TR-9542 ● SEP 2022

DEVCOM ARMY RESEARCH LABORATORY

A Novice's Guide to Approximating the Material Stresses and System Requirements for Hypersonic Flight

by Thomas Parker

NOTICES

Disclaimers

The findings in this report are not to be construed as an official Department of the Army position unless so designated by other authorized documents.

Citation of manufacturer's or trade names does not constitute an official endorsement or approval of the use thereof.

Destroy this report when it is no longer needed. Do not return it to the originator.

ARL-TR-9542 ● SEP 2022

A Novice's Guide to Approximating the Material Stresses and System Requirements for Hypersonic Flight

Thomas Parker
DEVCOM Army Research Laboratory

REPORT DOCUMENTATION PAGE

Form Approved
OMB No. 0704-0188

1. REPORT DATE *(DD-MM-YYYY)*	2. REPORT TYPE	3. DATES COVERED (From - To)
September 2022	Technical Report	October 2021–August 2022

4. TITLE AND SUBTITLE
A Novice's Guide to Approximating the Material Stresses and System Requirements for Hypersonic Flight

5a. CONTRACT NUMBER

5b. GRANT NUMBER

5c. PROGRAM ELEMENT NUMBER

6. AUTHOR(S)
Thomas Parker

5d. PROJECT NUMBER

5e. TASK NUMBER

5f. WORK UNIT NUMBER

7. PERFORMING ORGANIZATION NAME(S) AND ADDRESS(ES)
DEVCOM Army Research Laboratory
ATTN: FCDD-RLW-ME
Aberdeen Proving Ground, MD 21005

8. PERFORMING ORGANIZATION REPORT NUMBER
ARL-TR-9542

9. SPONSORING/MONITORING AGENCY NAME(S) AND ADDRESS(ES)

10. SPONSOR/MONITOR'S ACRONYM(S)

11. SPONSOR/MONITOR'S REPORT NUMBER(S)

12. DISTRIBUTION/AVAILABILITY STATEMENT
Approved for public release: distribution unlimited.

13. SUPPLEMENTARY NOTES
ORCID ID: Thomas Parker, 0000-0002-6151-6815

14. ABSTRACT

This report covers some of the material stresses and challenges in delivering a 155-mm munition at hypersonic speeds to long ranges (e.g., 100 km). The necessity of using slender bodies to reduce drag forces is discussed. Also considered is the explicit need for propulsion to maintain hypersonic speeds and the current performance limitations of solid rocket fuels. The high temperatures and heat fluxes, as well as the probable need to remove heat from the system to prevent excessive temperatures in the entire munition, are examined. The use of water to remove heat and act as a rocket fuel component and a mechanism to throttle a solid rocket engine is suggested as an avenue for future research. The recent development of an artillery shell gun launch with a solid fuel ramjet points to the need to develop solid rocket fuel chemistries that do not contain oxidizer and/or can utilize water vapors as a fundamental technological hurdle to overcome. The equations approximating the mechanical forces and heat-related stressors are given such that a non-expert could readily estimate the stresses for other flight systems and ranges.

15. SUBJECT TERMS
hypersonic, high temperature, erosion, solid rocket fuel, high heat flux, Science of Extreme Materials, Weapons Sciences

16. SECURITY CLASSIFICATION OF:			17. LIMITATION OF ABSTRACT	18. NUMBER OF PAGES	19a. NAME OF RESPONSIBLE PERSON
a. REPORT	b. ABSTRACT	c. THIS PAGE			Thomas Parker
Unclassified	Unclassified	Unclassified	UU	25	19b. TELEPHONE NUMBER (Include area code) (410) 306-0870

Contents

List of Figures

1. Introduction

The flow fields around a flight vehicle at hypersonic speeds are markedly different from those at both subsonic and supersonic speeds. The hypersonic regime is not at a discrete speed but evolves over a continuum as speed increases, but is generally defined as a speed of Mach 5 or higher. The flow fields around a vehicle cause the resultant high temperatures and high heat fluxes for the flight system/materials during hypersonic flight, and these stressors in hypersonic flight are called "The Heat Barrier." "Real gas effects" come into play at hypersonic speeds due to these high temperatures, and include vibrational excitation, dissociation, chemical reactions, and ionization. The underlying cause of this change in the flow fields is that the pressure waves created by the body moving through the atmosphere can only travel at the speed of sound. It is these pressure waves that travel ahead of the body and shape the flow field far from the body of a subsonic vehicle. At hypersonic speeds, the pressure waves have virtually no time to propagate away from the flight body, creating a condition where the pressure waves stack up very close to the flight body. These stacked up pressure waves form a bow shock very close to the flight body, where viscous heating occurs due to shear forces. These high-temperature gases close to the flight body surface lead to the high heat fluxes and high surface temperatures found in hypersonic flight.

The flow fields near the surface are plagued by nonequilibrium and/or chaotic thermodynamic conditions, where the temperature of the surfaces affects the flow field, thus affecting the temperature and so on. The problem of hypersonic flight is an exceedingly complex dynamic process, in that there is an interplay among the chemical changes to the surfaces, the changes in emissivity, surface temperatures, impact damage, and the flow fields, which all interact and feed back on one another. Although computer modeling has made great advances, this interplay cannot be accurately modeled currently. Also, there are no experimental facilities that can simulate all the flow conditions that are experienced during hypersonic flight. Even in cases where the flight conditions can be achieved, it is well known that the acoustic noise from the walls of the wind tunnel can alter the formation of shock waves. This results in increased turbulent flow on the different areas of the surfaces being tested depending on how these acoustic waves interfere, constructively or destructively. This can increase turbulence and lead to greater heat transfer (aerodynamic heating) than what would be found in the same structure in an atmospheric test flight.

Manufacturing variations can also lead to changes in the gas flow over surfaces and alter localized aerodynamic heating creating unexpected hotspots. The ablative heat shield tiles on the shuttle had to be hand mounted to insure an exacting degree of

uniformity. It was found that the protrusion of a single tile by as little as 1 mm would result in distortions of the shock wave downstream and resulted in unexpected hot spots that caused significant changes in the ablation rates of the tiles.

This should make clear that the conditions along the surface of a hypersonic body are specific to that object's geometry and defects. Further, even the ablation process itself can lead to sufficient structural changes that alter the gas flow over the surface, thereby altering the deposition of heat to the structure, which in turn alters the ablation rates, thus requiring intensive computer modeling and, in particular, actual flight testing to truly evaluate how a particular design will perform.

2. The Mach Cone

In 1936, Maccoll[1] conducted experiments to image the Mach cone of anti-tank rounds traveling at supersonic velocities. Some of the photographs captured by Maccoll are shown in Fig. 1. In the image on the top left, labeled Mach 1.06, the bow shock wave can be clearly observed to be out in front (left) of the point of the anti-tank round. There is a significant separation between the shock wave and the tip of the round. Also, the large radius of curvature of the shock wave results in a large volume of air in between the anti-tank round and the shock wave. In the next photo (top right), labeled Mach 1.16, the bow shock appears very close to the apex of the round. In addition, the radius of curvature has significantly decreased in comparison with Mach 1.06 and the shock wave has taken on the shape of a very blunt cone. With the progression to higher speeds, the angle of the bow shock, to the axial direction of the round, continues to decrease from Mach 1.231 to Mach 1.321 and then to Mach 1.576. Finally, at Mach 1.794, we see the smallest angle of the bow shock to the round's axial direction.

Figure 2 show the annotated photo of the anti-tank round at Mach 1.794. The tilting angle (θ) of the bow shock is with respect to the centerline (dashed white line) of the anti-tank round. The components of the free stream velocity (V_∞) are shown, where V_{Perp} is the component perpendicular to the shock front and V_{Par} is the component along or parallel to the shock front.

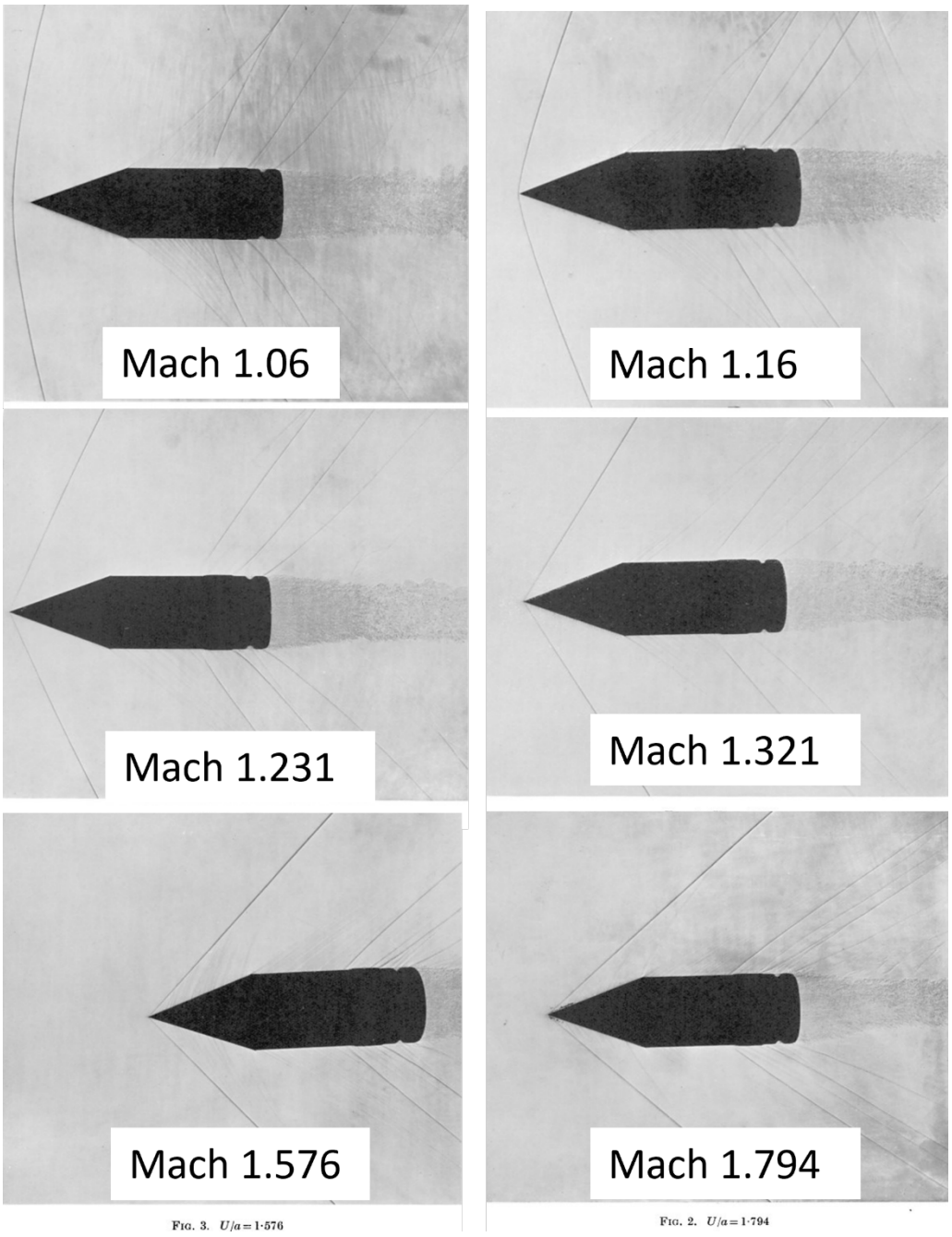

FIG. 3. $U/a = 1{\cdot}576$

FIG. 2. $U/a = 1{\cdot}794$

Fig. 1 Images of bow shock at different speeds of an anti-tank round

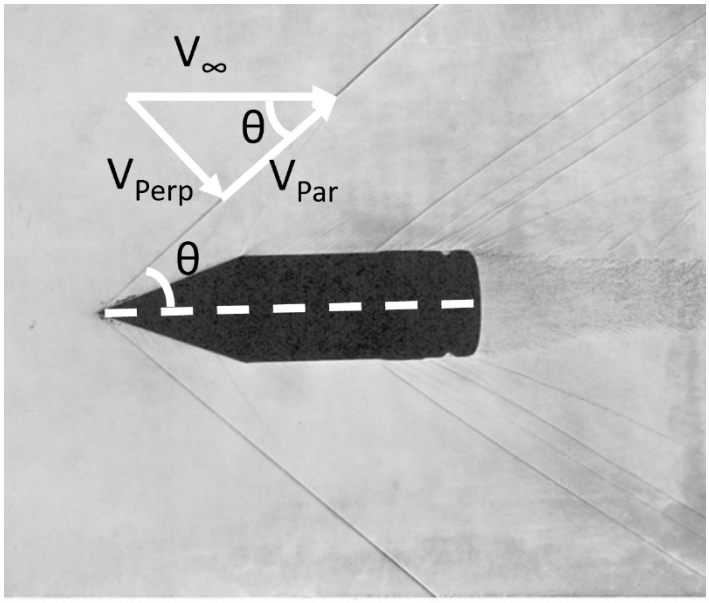

FIG. 2. $U/a = 1{\cdot}794$

Fig. 2 Annotated image of bow shock at Mach 1.794 showing the bow shock angle and components of free stream velocity

The angle at which the perpendicular component (V_{Perp}) is equal to Mach 1 is the angle at which the Mach cone or shock front forms. In Eq. 1, the angle (θ) of the Mach cone can be solved for a given free stream velocity (V_∞), where V_{Perp} is set to 1. This equation for the shock front cone angle is applicable to slender bodies.

$$\theta = sin^{-1}\left(\frac{V_{perp}}{V_\infty}\right) \quad (1)$$

For the case of the projectile in Fig. 2 with a free stream velocity of Mach 1.794, the predicted Mach cone angle is 49.2°. From a cursory visual inspection, one can readily see that this is in reasonable agreement with the experimental angle of the shock wave in Fig. 2.

This decreasing tilt of the Mach cone with increasing free stream velocity is a major factor in driving the characteristics of hypersonic flight, specifically aerodynamic heating. In Fig. 3, a plot of Eq. 1 is shown where the x-axis is the Mach number and the y-axis is the respective Mach cone angle (as shown in Fig. 2). As hypersonic speeds are attained, the Mach cone angle becomes very small. For a slender body at Mach 5, the Mach cone angle is predicted to be 11.5° from Eq. 1. Clearly at the speed of Mach 5, the Mach cone or shock wave will come very close to the surface of the projectile. This causes a trapped region of gas between the shock wave, where gases are decelerated (heated), and the body of the projectile. The stagnation temperature of this gas tends to be very high at hypersonic speeds. The close

proximity of these hot gases, and the resultant heat load, to the flight vehicle is the main material and engineering challenge to hypersonic flight.

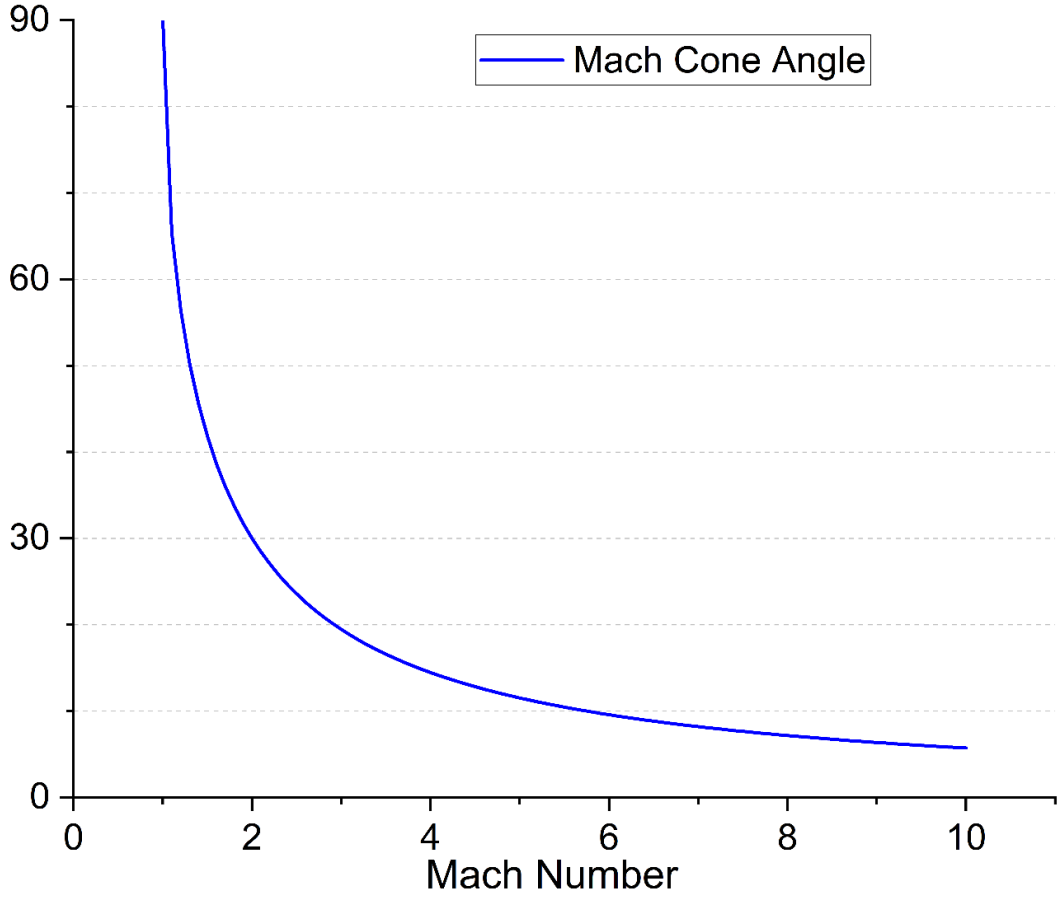

Fig. 3 Plot of the Mach cone angle as a function of Mach number

In 1957, Hodges[2] conducted hypersonic experiments measuring drag forces of spheres. In Fig. 4, an image of a 3/8-inch-diameter sphere traveling at Mach 9.5 from Hodges' work is shown. The shock wave is in very close proximity to the surface of the sphere. A large percentage of the sphere's surface area is enveloped by the shock wave. In these experiments, the spheres experienced significant mass loss due to the high temperatures caused by aerodynamic heating at this high Mach number.

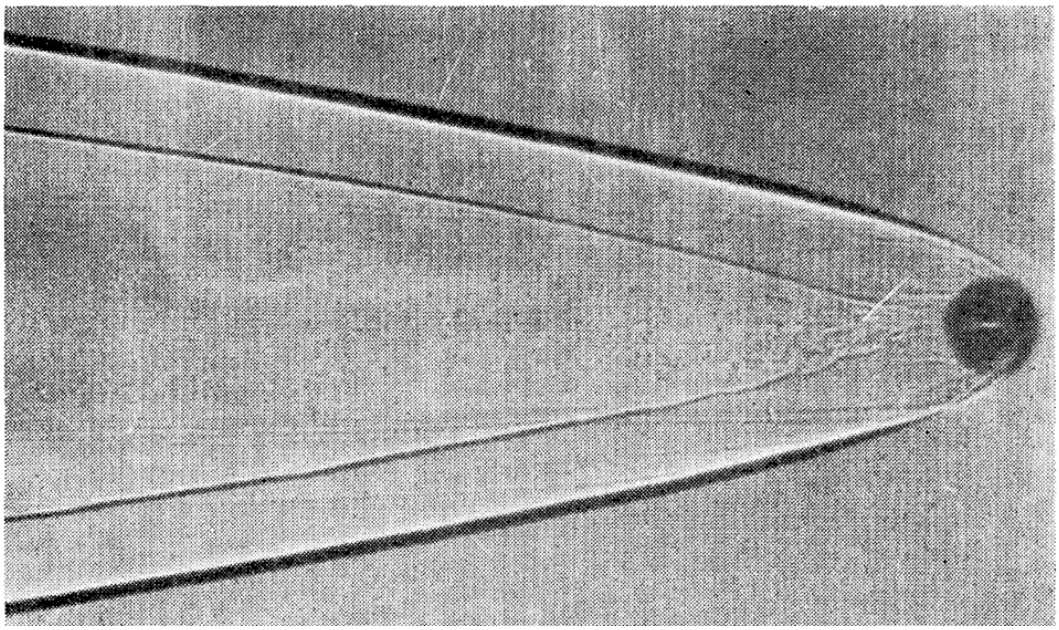

Fig. 4 Image of bow shock of a sphere at Mach 9.5

At sub-Mach speeds, the drag force is dominated by frictional drag. For Mach numbers greater than Mach 1, the drag forces are dominated by wave drag and shock-induced boundary layer separation.

3. The Drag Force

The drag force (F_D) is given in Eq. 2. The first term is the coefficient of drag (C_D). It is dimensionless and dominated by wave drag at hypersonic speeds. The cross-sectional area (A) is in units of meters squared, the velocity of the free stream (V_∞) in meters per second, and the free stream density of the atmosphere (ρ_∞) in kilograms per cubic meter.

$$F_D = \frac{1}{2} C_D A V_\infty^2 \rho_\infty \tag{2}$$

The coefficient of drag for a sphere decreases from a value of approximately 0.98 at Mach 2 to approximately 0.92 at Mach 5.[3] In Eq. 3, one can see the equation for the coefficient of drag (C_D) for a cone as a function of cone angle (ε), where ε is the angle from the cone's centerline to its edge. Consequently, the sharper a cone, the lower the C_D. For example, a cone with an ε of 10° will have a C_D of 0.06. This is approximately a factor of 20 lower than a that of a hemisphere (C_D = ~1).

$$C_D = 2sin^2\varepsilon \tag{3}$$

For the purpose of understanding the order of magnitude of the drag force at hypersonic speeds, a C_D of 1 may be used, as this is the approximate value for a hemisphere. It should be noted that C_D is a function of speed, and the value of C_D for a sphere decreases at Mach 5 and above to approximately 0.9. However, these changes in C_D with speed have relatively little effect on the force of drag in comparison with changes in the free stream velocity. What should be clear is that the drag force for an object with a given speed is approximately 100 times smaller at 30 km versus at sea level.

The altitude that an artillery piece attains is dependent on the firing angle; a typical altitude that a piece of artillery will reach is on the order of 10 km. In Fig. 5, a plot of the density of the atmosphere versus the altitude is shown. Along the x-axis is the altitude in kilometers and the corresponding density is given on the y-axis in kilograms per cubic meter. As can be seen in the graph, an altitude of 10 km corresponds to a density of approximately 0.4 kg/m^{3}r. An artillery projectile would obviously be fired from a much lower altitude than 10 km. Ideally, the firing charge would be used to bring the projectile up to 10 km at sub-hypersonic speeds, thus limiting the thermal load and drag at the lower altitudes. This is important as solid rocket engines are not able to be throttled to lower power and speeds. Then, the rocket engine would be ignited at 10 km and the flight path where the rocket is maintaining hypersonic speed can be fixed at 10 km. This greatly simplifies the problem of estimating the rocket requirements. If the projectile is to be considered hypersonic, then a speed of Mach 5, or approximately 1500 m/s, is generally accepted as the minimum to meet this definition. A projectile with a 155-mm diameter is a standard sized munition used by DOD and NATO partners and therefore an applicable example to explore. The cross-sectional area can be readily calculated, yielding a value of approximately 1.88E-2 m^2. Multiplying the previous values together yields a drag force of approximately 8.5 kN, or approximately 1,900 lb of force throughout the hypersonic flight resisting the motion of a projectile with hemispherical front surface.

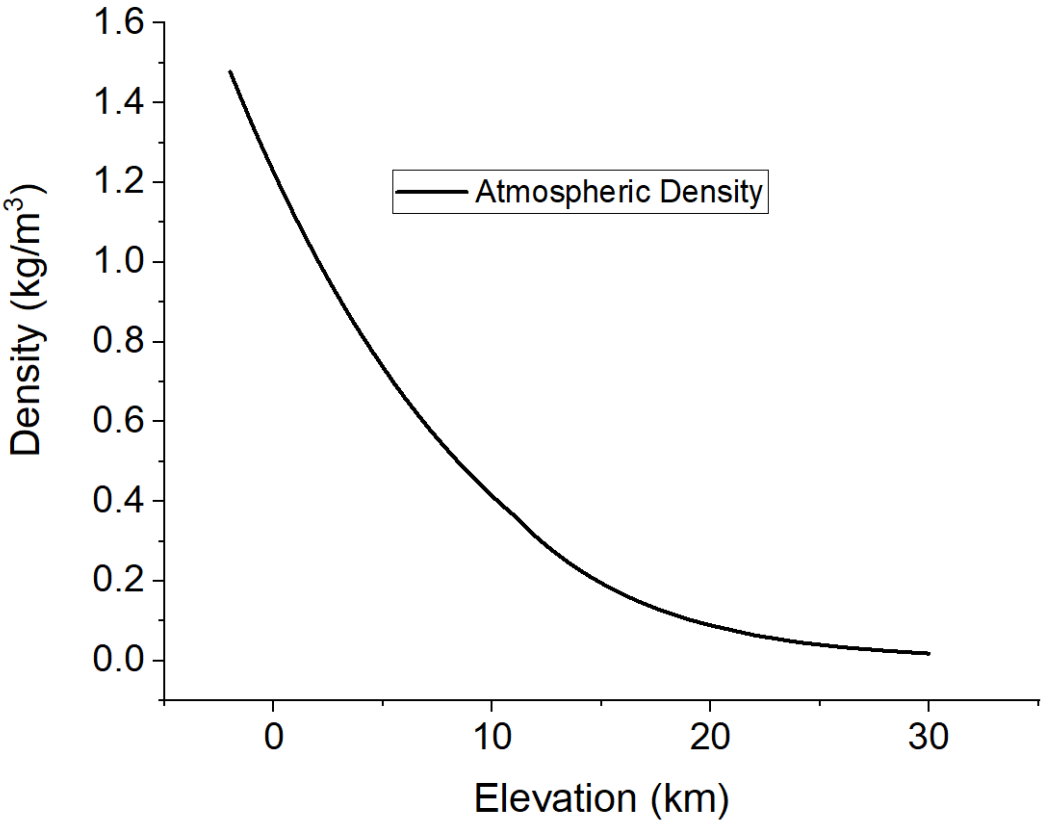

Fig. 5 Plot of atmospheric density vs. elevation

If a sharp cone was used instead of a sphere, the force would be reduced by a factor of approximately 20, as given by Eqs. 2 and 3 for a 10° cone, resulting in a drag force of 0.5 kN, or 115 lb of force. As an aside, the force experienced during a gun launch of a hypersonic projectile will likely far exceed the drag force in either case, so in principle, the aerodynamic pressure on the structure should be of no concern to the mechanical integrity of the vehicle. However, the materials supporting these aerodynamic loads can reach high temperatures, which lead to a significant reduction in the fracture toughness and hardness. Returning to the drag force, if we consider the sphere a worst-case scenario and the cone a best-case scenario, the actual drag experienced by a projectile will likely lie somewhere between these extremes. For example, a sharp cone may undergo sufficient aerodynamic heating and erosion that the cone becomes blunted during flight due to material loss, thus resulting in an increasing coefficient of drag and drag force. This idea of in-flight blunting is only mentioned in passing for awareness and is not explored further.

For a projectile to maintain a constant speed in the face of the drag force, an equal and opposite force is needed (i.e., propulsion). As rocket engines are currently integrated into extended-range artillery shells, a solid rocket engine is the likely

source of propulsion for a hypersonic gun launch projectile. Liquid fuel rockets do have significantly better performance than solid fuel rockets; however, the greatly increased complexity of liquid fuel rockets and the associated costs may make them cost prohibitive. In addition, the risk and logistic issues with liquid fuels such as cryogenic liquid oxygen or hydrogen and the associated risk of explosion would make liquid fuel rockets a highly complex and dangerous approach to gun launch hypersonics. In Eq. 4, the force of a rocket is shown as the product of the ejection velocity of the rocket propellant (v) and the rate of rocket fuel mass being used (dm/dt). The drag force is by far the majority force acting on the projectile and also requires the majority of the energy input into the projectile.

$$F_R = v\frac{dm}{dt} \tag{4}$$

We set the force of the rocket equal to the drag force on a projectile at 1500 m/s (i.e., 8.5 kN). The exhaust velocity of ammonium perchlorate composite propellant (APCP) is used as a benchmark with an exhaust velocity of approximately 2800 m/s. Knowing the propulsive force from the rocket and the exhaust velocity, the amount of mass ejected by the rocket per unit time can be determined to be 3 kg/s for the case of a hemispherical nose cone. Alternatively, a very sharp cone could be used with an ε equal to 10° and would result in the drag force being reduced by a factor of approximately 20 to approximately 0.5 kN of rocket thrust needed to overcome the drag force, with a corresponding reduction in the mass ejection rate to approximately 0.183 kg/s.

What does this mean within the realm of future Army goals? A goal for future generations of long-range artillery is the ability to deliver a projectile at distances on the order of 100 km. With a speed of 1500 m/s, this would result in a flight time of approximately 66 s. As shown in the earlier, a projectile with a hemispherical nose would need a rocket that would expend 3 kg/s to overcome the drag force encountered by a 155-mm projectile traveling at 1500 m/s. For this projectile to travel 100 km at 1500 m/s, a significant amount of rocket fuel would be needed. Multiplying the mass expenditure rate (3 kg/s) times the flight time (66 s) would yield a total weight of rocket fuel on the order of 202 kg. A typical artillery shell weighs on the order of approximately 45 kg. This should be considered close to an upper limit, as much heavier projectiles would be difficult for Soldiers to pick up/handle and load. It should be obvious that a gun-fired projectile requiring 202 kg of rocket fuel is not feasible. This is without adding any additional weight for the rocket engine itself and other components.

Another issue is that rocket fuel is low density, at most, approximately 2000 kg/m^3 but usually lower, and the volume needed to contain 202 kg of material is huge in

the context of an artillery shell. One of the highest performance solid rocket fuels in open literature was developed by the Navy, hexanitrohexaazaisowurtzitane (Cl-20). The density of CL-20 is 2.04 g/cm^3 and it yields a much higher volume efficiency (~+20%) than other solid propellants. Using the density of CL-20, this would result in a volume of approximately 0.101 m^3 being required to hold 202 kg of propellant. The volume of a cylinder is given by its length L times the cross-sectional area, where the cross-sectional area is just the radius squared times π. For a cylinder with a radius of 0.0775 m (e.g., a 155-mm shell), a cylinder would have to be 5.35 m in length. Again, this is unreasonable and would not be feasible in a fieldable artillery device with a 155-mm diameter. The logistics of transporting artillery shells that are approximately 5 m in length would be prohibitively difficult and costly.

If the design of a shell were altered to instead utilize a sharp cone geometry, a significant reduction in drag could be realized and consequently the amount of thrust and rocket fuel needed. If a sharp cone has an ε equal to 10°, the drag force and required rocket thrust would be reduced by a factor of approximately 20. However, at an angle of 10°, the height of a cone with a radius of 0.0775 m is 0.435 m, meaning that almost the entire length (0.6 m) of a 155-mm shell would consist of this very narrow cone. If we assume that a cone this narrow could be integrated into an artillery shell, the resulting reduction in drag coefficient leads to an approximately 20 times decrease in the required rocket fuel mass flow (e.g., 0.183 kg/s). For a 66-s flight, this would require the rocket to expend 12.2 kg of fuel, corresponding to a fuel volume of 0.006 m^3 for CL-20. Again, one should note this 12.2 kg due to rocket fuel does not include the weight of the artillery shell/structure, gun propellant, electronics, or any of the rocket structure/ components, and assumes the rocket is 100% efficient. The length of a 155-mm tube needed to accommodate a rocket fuel at a density of 2000 kg/m^3 is reduced to a much more reasonable 0.32 m; however, this still takes up over half the length of current 155-mm shells at approximately 0.6 m.

Improvements in solid rocket fuel energy density per unit mass and per unit volume will have to increase drastically to come close to the form factor and weight of current 155-mm shells. A solid rocket fuel with an exhaust velocity of 4000 m/s would reduce the mass of the rocket fuel required to transit 100 km at Mach 5 to 0.04 kg/s, or a total of 8.5 kg of rocket fuel. It should be clearly stated that this would require a huge improvement (42%) in exhaust velocity over APCP's exhaust velocity of 2800 m/s. A cylinder with a diameter of 155 mm and a length of 0.6 m has a volume of approximately 0.0113 m^3. To occupy 25% of this volume with 8.5 kg of rocket fuel would require a rocket fuel with a density of a little over

3000 kg/m^3, or a 50% improvement over CL-20 at 2040 kg/m^3, which is one of the highest energy density solid rocket fuels yet developed.

4. Aerodynamic Heating

The ideal gas law is shown in Eq. 5, where P is the pressure; V is the volume; n is the number of mols; R is the ideal gas law constant, which is the product of the Boltzmann constant and Avogadro's number; and finally T is the temperature:

$$PV = nRT \tag{5}$$

The ideal gas law is derived by assuming a gas has 3 degrees of freedom. Shock-induced heating that occurs during hypersonic flight causes the gases to deviate from this law. The underlying cause is the fact that R is dependent on Boltzmann's constant. Implicit in the calculation of Boltzmann's constant are the degrees of freedom that a gas molecule has and consequently the number of quantum mechanical energy states available (or the density of states) the gas molecules can occupy. The shock-induced temperatures and frictional forces that gases undergo during hypersonic rates raise the kinetic energy high enough to enable additional degrees of freedom, specifically the vibrational modes of the diatomic gas are activated. This means that the heat capacity of the gas is not constant but changes due to the additional energy states available. These vibrational states are initially activated in the Mach 3 to 4 range and lead to measurable deviations from the ideal gas law at hypersonic speeds. This increased ability to carry heat consequently leads to an increased heat transfer to the flight body.

In the Mach 9 range at altitudes in the lower stratosphere (~10,000 m) range, oxygen dissociation begins to take place. This oxygen dissociation is also referred to as one of the "thermochemical effects." At speeds around Mach 16, another thermochemical effect begins to take place, nitrogen dissociation. At this point, both oxygen and nitrogen radicals can land on surfaces and cause thermochemical-induced reactions with the surfaces. Finally, at speeds near Mach 30, plasma will begin to form a conductive sheath around the flight object. This plasma sheath has sufficient electrical conductivity to act as a Faraday cage, leading to the blocking of both the transmission and receipt of electromagnetic communication signals (i.e., a "blackout"). Additionally, plasma has a wide array of radical atomic and molecular species that can lead to intense attack of surfaces. As we are limiting our discussion to speeds in the range of Mach 5, these more exotic hypersonic effects are not discussed further; however, the temperatures at hypersonic speeds still pose a significant stressor to materials exposed to them.

Additionally, chemical processes such as high temperature oxidation are still a significant issue at Mach 5. In Eq. 6, the stagnation temperature (T_S) is given as a function of the ambient temperature T, the Mach number, and the ratio of the heat capacities γ, which for calorically perfect gases has a value of 1.4. The temperature scale used should be in Kelvin to make the calculation.

$$T_S = T\left[1 + \frac{\gamma - 1}{2} M^2\right] \tag{6}$$

At an altitude of 10 km, the ambient temperature T is on the order of 233 K, or –40° C. We can solve for the stagnation temperature at Mach 5 in the case of a calorically perfect gas given a temperature of 1125° C. The equation for a calorically imperfect gas is included if the reader would like to make a more exacting estimation of the stagnation temperature.

In Eq. 7, the ambient temperature is given by T; the Mach number by M; the gamma (γ) is the ratio of heat capacities, which is 1.4; and theta (θ) is a thermal constant with a value of 5500° Rankine; the non-caloric correction term γ_{NC} is given in Eq. 8. To solve for the stagnation temperature, the equations must be solved recursively where a stagnation temperature is input and the Mach is solved for, then changing the stagnation temperature up or down to achieve the desired Mach number. At very high (>10) Mach numbers, the deviation from a calorically perfect gas can be significant, hundreds of degrees Celsius lower (or more) than the calorically perfect gas. However, in the lower hypersonic range, the deviation is on the order of 50 °C or less.

$$M^2 = \left[\frac{2\frac{T_S}{T}}{\gamma_{NC}}\right]\left[\left(\frac{\gamma}{\gamma - 1}\right)\left(\frac{1}{\left(\frac{T}{T_S}\right)} + \frac{\theta}{T_S}\right)\left(\frac{1}{e^{\frac{\theta}{T_S}} - 1} - \frac{1}{e^{\frac{\theta}{T} - 1}}\right)\right] \tag{7}$$

$$\gamma_{NC} = 1 + \frac{\gamma - 1}{1 + \left((\gamma - 1)\left(\frac{\left(\frac{\theta}{T}\right)^2 e^{\frac{\theta}{T}}}{e^{\left(\frac{\theta}{T} - 1\right)^2}}\right)\right)} \tag{8}$$

The heat flux (φ_w), in watts per square meter, to the wall of the flight vehicle during hypersonic flight can be approximated by Eq. 9, where ρ_∞ is the density of the free stream, the density of the atmosphere at a given altitude. The free stream velocity is given by V_∞, and κ is a heat transfer coefficient and can be approximated[4] as 10^{-2}.

$$\varphi_w = \kappa \rho_\infty V_\infty^3 \tag{9}$$

The density of the atmosphere at 10 km is 0.4135 kg/m^3. At Mach 5 (or 1500 m/s), the heat flux per square meter is 14 MW/m^2. For a 155-mm projectile with a 10° cone, the wetted area (surface area of cone) is 0.126 m^2, yielding 1.76 MW. Over the course of a 66-s flight, the total heat energy absorbed by the flight body is 116 MJ. If this heat energy is left to sit in the flight body, the body would experience large temperature rises. If we assume that the artillery has a heat capacity of 2000 J/kg-°C with a weight of 50 kg, the resultant temperature rise would be Δ1159 °C. This estimate is a gross oversimplification, as some of this heat will be reradiated by the hotter surfaces of the flight body and the heat transfer rate will decrease as the wall temperature increases. But it still is useful, in that it points out the need to remove the absorbed heat. Research into modifications, such as doping hot surfaces like leading edges, could help reduce the maximum temperature of these leading edges as well as remove heat. The leading-edge materials need to have a high thermal conductivity to avoid the harsh thermal shock conditions. This high thermal conductivity will result in heat being transported to much cooler areas and possibly sensitive areas such as the solid rocket fuel, electronics, and so on. These areas will not radiate nearly as much thermal energy until very hot due to the radiated power varying proportionately to the temperature to the fourth power.

Other means to remove heat will be needed to protect the majority of the flight body from high temperatures. One example of an approach to remove heat was used by the SR-71. The SR-71 would be flown below cruise speed at altitude to super cool the JP-7 jet fuel in the fuselage. This supercooled fuel would then be used to lubricate and cool the internal engine burn areas during high-speed (Mach 3) flight where the JP-7 would reach several hundreds of degrees Celsius before being injected into the engine and burned. If a similar approach was used to dissipate heat in a gun-fired projectile, one could imagine using vaporizing water to remove the heat from the flight system. The heat of vaporization for water is 2.257 MJ/kg. Therefore, to remove all the absorbed heat, one would need to vaporize approximately 50 kg of water during flight. This is an overestimate of water needed but has the correct order of magnitude.

Additionally, could this water serve multiple purposes? The injection of water into a solid rocket engine has been shown to increase burn efficiency and therefore reduce the amount of solid propellant needed.[5] This may be an avenue worth investigating, as vaporized water carrying heat out of the body of the flight vehicle could be injected into the rocket engine chamber thus increasing the propellant efficiency. The development of propellant chemistries to explicitly utilize water may be a useful field to investigate. Another concept that may be interesting is the

fact that solid rocket engines with a single chemistry cannot be throttled in flight like liquid rocket engines. Varying the amount of water being injected could be an avenue for altering the thrust in flight to vary speed. An artillery round must come down somewhere, and traveling at Mach 5 at or near sea level leads to approximately 3.5 times (430 MW/m^2) the heat flux versus that at 10 km.

An exciting new demonstration by Boeing and Nammo[6] involved the gun launch and subsequent ignition of a ramjet within a 155-mm artillery shell. This ramjet utilizes a solid rocket fuel and is designed to fly at Mach 3. One of the challenges of increasing a ramjet speed further is that the surfaces within the ramjet are subject to extreme temperatures as hypersonic gases are compressed. Gas shrouds have been used to shield components from the intense heat during hypersonic flight. The ability to inject a gas shroud such as water vapor (also carrying away heat from the body as mentioned previously) could help protect components within the ramjet as well as serve to increase the solid rocket fuel efficiency.

Optimizing solid rocket fuel chemistries for ramjet operation and/or water vapor injection would likely prove instrumental in achieving long-distance hypersonic gun launch. Removing the need to carry the oxidizer within the solid fuel opens up new avenues for possible rocket fuel chemistries. These chemistries would need to improve significantly in both mass and volume efficiency over current cutting-edge solid rocket fuels. It should be noted that a ramjet loses thrust and efficiency much above Mach 5 and a scramjet instead would be needed for higher speeds.

5. Erosion

At hypersonic speeds, the kinetic energy in a collision between vehicle surfaces and dust/raindrops can result in erosion due to impact damage. A theoretical equation for the damage threshold velocity from Evans et al.[7] is given in Eq. 10. The factor toughness is K_{Ic}, the Rayleigh surface wave speed c_R, density of water ρ_w, the compressive wave speed of water $c_w = 1500$ m/s, and the diameter of the raindrop $d_w = 1.5$ mm.

$$V_{threshold} = \left(\frac{{K_{Ic}}^2 c_R}{\rho_w^2 c_w^2 d_w} \right)^{1/3} \tag{10}$$

In Eq. 11, the formula for the Rayleigh surface wave speed is given, where the Poisson's ratio for the surface material is given by v, the Young's modulus by E, and the density by ρ.

$$c_R = \left(\frac{0.862+1.14\nu}{1+\nu}\right)\sqrt{\frac{E}{2(1+\nu)\rho}} \tag{11}$$

Monteverde et al.[8] examined the mechanical properties of zirconium diboride–silicon carbide (SiC) matrix composites. The density of the composites was found to be between 5.51 and 6.09 g/cm^3 dependent on the SiC weight percent (5 to 20 wt%). The modulus E was found to be between 518 and 477 GPa, the factor toughness was between 4.49 and 5.42 MPam$^{1/2}$, the hardness was between 19.3 and 21.7 GPa, and Poisson's ratio was between 0.103 and 0.117. Using the 20 wt% SiC data, the Rayleigh wave speed calculated using Eq. 11 is 1755 m/s. This Rayleigh wave speed can then be plugged into Eq. 10 to yield a damage threshold of 230 m/s. The velocity at Mach 5 of 1500 m/s is well above this threshold damage velocity and consequently there will be erosion.

It should be noted that at these high Mach numbers, as a droplet transits the shock wave, it will tend to dissipate due to sheer forces and heating. Droplets will also tend to become elongated perpendicular to the direction of motion, becoming disc-like and spreading any force out over a larger area thus reducing damage. Additionally, the angle between the water disc and the projectiles surface will affect the area the impacting disc is spread out over as well as reduce the normal component of the impact force. This indicates that a leading edge that is very "sharp" will suffer less impact damage.

On the materials side, the fracture toughness is given in Eq. 12, where a constant δ is equal to approximately 0.016, E is the Young's modulus, H is the hardness, P is the load of the indentor being used, and c is the measured crack length laterally from the center of the indentor. Both the Rayleigh surface wave speed and the fracture toughness contribute a square root of the modulus, resulting in a linear dependence of the damage threshold velocity on the Young's modulus. Stiffer materials will tend to perform better under the erosive environments found at hypersonic speeds.

$$K_{Ic} = \delta\sqrt{\frac{E}{H}}\frac{P}{c^{3/2}} \tag{12}$$

6. Conclusion

The challenges associated with hypersonic flight are significant in that the drag forces, temperatures, and heat flux put large demands on materials. First and foremost is managing the exposure to high temperatures that will be in excess of

1000 °C. The high heat flux to the flight body can result in very high temperatures of the entire vehicle during flight. Mechanisms to carry away heat, such as increased emissivity of leading-edge materials, should be explored. The use of cooling in the form of water vaporization may be a route that can be used to increase rocket fuel efficiency and provide a mechanism for throttling a solid fuel rocket. As the effects of erosion are unavoidable at hypersonic speeds, the use of materials with high Young's moduli could mitigate this effect.

7. References

1. Maccoll JW. The conical shock wave formed by a cone moving at a high speed. Proc R Soc Lond A. 1937;159:459–472.

2. Hodges AJ. The drag coefficient of very high velocity spheres. J Aeronaut Sci. 1957 Oct;24(10):755–758.

3. Masson DJ, Morris DM, Bloxsom DE. Measurements of sphere drag from hypersonic continuum to free-molecule flow. RAND; 1960. Report No.: RM-2678.

4. Urzay J. The physical characteristics of hypersonic flows (I), lecture 2, ME356 lnamics. Stanford University; 2021 https://www.youtube.com/playlist?list=PL04kBjbWQWOPYBfbw2zqnMbWHNjU3MDYB.

5. Prisniakov VF, Gabrinets VA, Markov VL, Petrov BE. Research of transient thermal characteristics of channel in high temperature energy storage. IAF International Astronautical Congress, 43rd; 1992 Aug 28–Sept 5; Washington DC. IAF-92-0636.

6. Nammo. Boeing, Nammo complete long-range ramjet artillery test. Nammo; 2021. [accessed 2022 Aug 12]. https://www.nammo.com/.

7. Evans G, Ito YM, Rosenblatt M. Impact damage thresholds in brittle materials. J App Phys. 1980;51:2473–2482.

8. Monteverde F, Guicciardi S, Melandri C, Dalle Fabbriche D. Densification, microstructure evolution and mechanical properties of ultrafine SiC particle-dispersed ZrB_2 matrix composites. In: Orlovskaya N, Lugovy M, editors. Boron rich solids. NATO Science for Peace and Security Series B: Physics and Biophysics. Springer, Dordrecht; 2010.

List of Symbols, Abbreviations, and Acronyms

APCP	ammonium perchlorate composite propellant
ARL	Army Research Laboratory
CL-20	hexanitrohexaazaisowurtzitane
DEVCOM	US Army Combat Capabilities Development Command
DOD	Department of Defense
NATO	North-Atlantic Treaty Organization
SiC	silicon carbide

1 (PDF) DEFENSE TECHNICAL INFORMATION CTR DTIC OCA

1 (PDF) DEVCOM ARL FCDD RLD DCI TECH LIB

31 (PDF) DEVCOM ARL
FCDD RLC P
C M BEDELL
FCDD RLS EM
H TSANG
FCDD RLW
J ZABINSKI
A RAWLETT
S KARNA
S SCHOENFELD
FCDD RLW M
E S CHIN
FCDD RLW MC
J F SNYDER
FCDD RLW MD
J LA SCALA
C M MOCK
J YU
A BUJANDA
FCDD RLW ME
T PARKER
L VARGAS-GONZALES
M IVILL
V BLAIR
K BEHLER
N KU
A DIGIOVANNI
W SHOULDERS
C HUBBARD
S G HIRSH
M GOLT
FCDD RLW MF
J P LABUKAS
J D DEMAREE
FCDD RLW WD
V BHAGWANDIN
J DESPIRITO
J PAUL
J SAHU
L STROHM
J VASILE